Waste and Biomass Valorization (2021) 12:5715–5723
https://doi.org/10.1007/s12649-021-01377-2

ORIGINAL PAPER

Chemical and Mechanical Properties of Films Made of Cellulose Nanoplatelets and Cellulose Fibers Obtained from Banana Pseudostem

G. Flores-Jerónimo[1] · J. Silva-Mendoza[2] · P. C. Morales-San Claudio[2] · A. Toxqui-Terán[3] · J. A. Aguilar-Martínez[1] · L. Chávez-Guerrero[1,4]

Received: 28 July 2020 / Accepted: 28 January 2021 / Published online: 19 February 2021

Abstract

Biopolymers arise as a good substitute for synthetic polymers, regardless of the energy demand and the complex processes required to isolate such biopolymers. Cellulose is an organic polymer that can be found in all terrestrial plants and is the most abundant organic biomolecule on the Earth. However, the mechanical properties of most biopolymers are not as good as the ones of synthetic polymers under environmental conditions, because they are highly hydrophilic. In this work, we aimed to extract cellulose nanoplatelets (CNP) and cellulose fibers (CF) from the banana pseudostem through one step of alkalinization followed by acid hydrolysis, to obtain a self-standing transparent film. The obtained all-cellulose material (CF/CNP) was characterized by Optic Microscopy, Scanning Electron Microscopy, Attenuates Total Reflection Spectroscopy, X-Ray diffraction. Also, CF/CNP films were made in order to test their tensile and strength properties, along with the simulated biodegradability using enzymatic hydrolysis.

Graphic Abstract

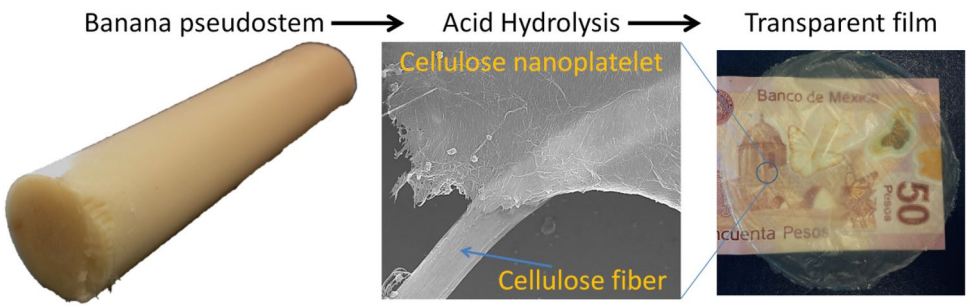

Keywords Two-dimensional nanocellulose · Microcrystalline cellulose · Thin films · Transparent films · Biopolymers

✉ L. Chávez-Guerrero
leonardo.chavezgr@uanl.edu.mx

[1] Facultad de Ingeniería Mecánica y Eléctrica, Universidad Autónoma de Nuevo León, Av. Universidad s/n, San Nicolás de los Garza, Nuevo León 66455, México

[2] Facultad de Ciencias Químicas, Universidad Autónoma de Nuevo León, Av. Universidad s/n, San Nicolás de los Garza, Nuevo León 66455, México

[3] Centro de Investigación en, Materiales Avanzados S. C. (CIMAV—Unidad Monterrey), Av. Alianza Norte 202, Autopista Monterrey-Aeropuerto Km 10, PIIT, Apodaca, Nuevo León 66628, México

[4] Centro de Innovación, Investigación y Desarrollo en Ingeniería, Universidad Autónoma de Nuevo León UANL, Av. Alianza 101 Sur Km. 10 de la Nueva Carretera Internacional de Monterrey, Apodaca, Nuevo León 66600, México

Statement of Novelty

Here we aim to demonstrate the importance of two-dimensional nanocellulose isolation to obtain a self-standing film, which can be considered an all-cellulose composite. The manuscript includes a wide study of the resulting mix of cellulose nanoplatelets and cellulose fibers by ATR and XRD. The morphological studies were analyzed by SEM and OM techniques, which lead to the findings of the presence of two-dimensional nanocellulose with nanoplatelet shape. A free-standing film made of cellulose fibers and cellulose nanoplatelets was successfully obtained; such films have a crystallinity index of 78 which can withstand up to 180 MPa. Also, we present preliminary results on the biodegradability of the cellulose films, showing that 50% of the material will be decomposed in 7 days due to the action of enzymes at the end of the useful life.

Introduction

Since the middle of the last century, polymers have become an indispensable material for the development of applications useful to society due to outstanding properties of elasticity, plasticity transparency and strength [1]. The aforementioned materials have become essential in a broad range of human applications, from industrial to domestic. However, the fossil resources from which they are made decreases constantly but demand keeps increasing and they will be depleted within the next one hundred years [1]. Furthermore, the lack of proper care of some polymers after utilization is driving this situation into an ecological problem of great relevance because such materials take a long period to fully degrade under environmental conditions [2]. Hence, there is an increasing demand for innovative routes and materials to obtain polymeric materials utilizing renewable resources. Utilizing renewable feedstocks such as biomass [3], for the generation of modern biodegradable plastics has environmental and financial benefits. Then, the field of non-petrochemical derived polymers draws attention in both a commercial and technological sense. These materials are the result of biochemical processes between CO_2, water and sunlight through photosynthesis which practically discards the use of fossil resources, which can be considered as neutral emission of carbon for their synthesis. Conveniently, these same biochemical processes (carried out by enzymes, such as cellulases and amylases) can be applied in reverse for the degradation of these biopolymers, since microorganisms can use them as a carbon source for obtaining energy, converting them back into carbon dioxide and water [4]. Unfortunately, biomass-based polymers do not have good mechanical properties in terms of strength and are difficult to process with the conventional equipment used with synthetic polymers [1]. In this context, lignocellulosic biomass, the most abundant and bio-renewable biomass on earth [5] plays an important role due to its abundance and the fact that it is available worldwide. Thus, cellulose rises as a promising substitute for fossil oil-based polymers due to its biocompatibility, renewability and biodegradability [6]. Many residues of the food industry have been studied as novelty sources of cellulose, among which are: *Agave salmiana* [7], Corn husk [8], *Opuntia ficus-indica* [9] and *Abelmoschus esculentus* [10].

Banana planting and harvesting occurs worldwide, mainly in tropical conditions where the fruit represents only 12% of the total mass of the plant [11]; the rest consists of leaves, peels, rachis, stalk, inflorescence, stem and pseudostem [12]. In 2019, global exports are expected to reach 20 million tons of banana fruit in their different varieties, having Asia and America 95% of the global production [13]. An important aspect to heed is that banana trees are perennial plants that are dismissed once the fruit is collected (single harvest) which could drive to important environmental issues, such as fungus and insects proliferation, if the residual biomass does not have adequate disposal. Banana pseudostems have an inner soft fibber wrapped by a coarse fiber at the external section, which has been utilized commonly in textiles production. The inner core is rich in nanocellulose which can be isolated in several ways, generally including three broad steps consisting of (1) pretreatment of the raw material, (2) hydrolysis supported by concentrated acids (≈ 63%) [14] followed by (3) defibrillation by TEMPO/ultrasonication [15, 16], mechanical milling [17, 18], steam explosion [19, 20] or enzymatic treatment [18].

There are several types of nanocellulose, but only three main groups are well recognized in literature, e.g. bacterial cellulose (BC), cellulose nanocrystals (CNCs) and cellulose nanofibrils (CNFs). Recently, a new morphology was reported, describing a two-dimensional (2D) nanostructure [21] known as cellulose nanoplatelets [22], which is easier to obtain and can be detected with help of an optical microscope, when such nanoplates were deposited on a silicon wafer. Nanocellulose films made of banana pseudostem nanoplates (2D) exhibited good transparency ≈ 83% [23], which make them candidates for several applications in the industry of packaging or food industry.

The synthesis of all-cellulose nanocomposites using banana pseudostems as a raw material is reported. This paper aims to produce films of cellulose fibers and nanocellulose to test their mechanical properties and biodegradability, to explore potential applications in the near future as a polymer substitute.

Materials and Methods

Materials

Sulfuric acid (98%), hydrogen peroxide (30%), and sodium hydroxide pellets were reagent grade and used without modification. The deionized water presents a resistivity of 18.1 MΩ m^{-1}. Microcrystalline cellulose (CMC) extracted from cotton (SigmaCell 20) was acquired from Sigma-Aldrich. Banana pseudostems from the species *Musa sapientum* were collected after harvest from the state of Nuevo Leon, Mexico. The inner banana pseudostems were cut into pieces of about 0.5 × 3 × 10 cm (thickness × width × length).

Mechanical Separation

The raw banana pseudostem specimens were put inside transparent plastic bags and frozen at − 50 °C for 12 h, then freeze-dried for 48 h until 80% of the water was extracted. Using a Bel-Art 37250 Micro-Mill Grinder, dried samples (15 g) were milled for 5 min to get fine powders which were sieved and named BI-Raw.

Cellulose Extraction

A mixture of 180 mL of deionized water, 20 mL of H_2O_2 (10% v/v) and 2 g of NaOH (1% w/v) were solubilized inside a conical flask. Later, 10 g of BI-Raw were added slowly to the flask and kept under constant stirring at 100 rpm for 60 min. Afterward, the dispersion was placed inside an autoclave at 110 °C and 0.5 kg/cm^2 for 40 min to promote the alkalinization/bleaching reaction. After that time, the autoclave was off and opened once the inside temperature come to 80 °C. The solid part of the dispersion was isolated by vacuum filtering and rinsed with deionized water three times to remove the remnant traces of NaOH; then H_2SO_4 was added drop by drop to neutralize the suspension (pH 7), and rinsed again to remove the remaining traces of acid. The obtained gel was used to produce films by solution casting method on a Petri dish drying the deposited solution in an oven at 40 °C for 48 h. In another set of experiments, the gel was dried in an oven and grounded in an agate mortar. The resultant samples, film and powder, were named BI-AT.

The hydrolysis was carried out by making a mixture of 130 mL of deionized water, 20 mL of H_2O_2 and 10 mL of H_2SO_4 (6.25% v/v) in a conical flask. 10 g of BI-AT powder, obtained by the method described above, were added to the flask and kept under constant stirring at 100 rpm for 60 min. Afterward, the dispersion was set within an autoclave at 110 °C and 0.5 kg/cm^2 for 40 min. When the time lapsed, the autoclave was off and opened once the inside temperature come to 80 °C. A white gel pulp was observed at the bottom of the flask and was separated by vacuum filtration and washed with deionized water three times. Next, an alkaline solution of NaOH was added drop by drop to neutralize the suspension (pH 7) and rinsed twice with deionized water to remove the remaining traces of salt [23]. The resulting gel, containing cellulose nanoplatelets and cellulose fibers was used to produce powders which were named BI-HT. Transparent films were made by the solution casting method, drying a suspension (10% w/v) of the hydrolyzed material on a Petris dish for 48 h at 40 °C.

Optic Microscope

A Leica light microscope DM 3000 model was used at 10×, 20×, and 50× to observe the samples at distinct scales.

Scanning Electron Microscope (SEM)

The tests were carried out in a scanning electron microscope FEI Nova NanoSEM 200, under high vacuum conditions with a secondary electron detector (ETD). The microscope was used at 5 kV, and a working distance of 5 mm. The samples were dispersed in ethyl alcohol, and then a drop of every sample was dried on silicon wafers at 40 °C for 2 h. The silicon wafers were glued to an aluminum pin and spin-coated with gold to enhance the surface conductivity. We use the program ImageJ to determine the diameter of the fibers (100 measurements) using SEM images.

Attenuated Total Reflection (ATR) Spectroscopy

The ATR spectra were recorded on a Nicolet 6700 spectrophotometer in the 4000–500 cm^{-1} range. Spectra were taken at a resolution of 2 cm^{-1}.

X-Ray Diffraction (XRD)

The samples were analyzed by X-Ray Diffraction, in a PANalytical powder diffractometer Empyrean model at room temperature operated at 45 kV, 40 mA. A Cu-Kα (λ = 1.5406 Å) radiation was used to gather the diffraction patterns within Bragg angle 2θ from 5° to 40°, using a step of 0.01° and a time step of 20 s. The crystallinity index *CrI* of samples was calculated using the Eq. (1), where I_{total} indicates the maximum intensity at the plane 200 (~ 22°) and I_{am} the minimum diffraction intensity at ≈ 18°, which represents the amorphous contribution [24].

$$CrI(\%) = \frac{I_{total} - I_{am}}{I_{total}} \times 100 \quad (1)$$

Tensile Tests

Uniaxial static mechanical stress tests were performed using a dynamic mechanical analyzer (DMA Q800, TA Instruments, New Castle, DE). For such tests (in triplicate), the film samples were cut into strips 5.3 mm wide by 10.5 mm long and 180–50 µm thick and mounted using film tension clamps. Tension tests were executed at 28° C in controlled force mode, with a preload of 0.01 N, and a force loaded on ramps of 0.5 N/min.

Biodegradability Test

Films were subjected to enzymatic degradation with a commercial enzyme mix (Celuzyme ®) derived from *Trichoderma longibrachiatum* at an enzymatic loading of 10 wt%. The enzymatic reactions were carried out in 15 ml conical tubes containing 300 mg of the cellulose film, 30 mg of enzyme mix (114,400 CMCase/g and 30,000 BGU/g), and 10 ml of 50 mM sodium acetate buffer (pH 5). Tubes were incubated at 35 °C and 150 rpm for 0, 1, 3, 4, 5, 6, and 7 days. After hydrolysis, tubes were boiled for 5 min to inactivate the enzymes and subsequently centrifuged at 4,500 rpm for 10 min. The reducing sugars were determined in the supernatant for 3,5 DNS acid method [25].

Results and Discussion

Microscopy Imaging

The three samples were analyzed by optic microscopy and the images are shown in Fig. 1. The raw material exhibits a series of rib-like structures. When raw fibers are subjected to alkaline treatment, the fibers seem to be randomly oriented caused by the partial breaking of lignin and pectin that are wrapping the cellulose [23]. Furthermore, when the acid treatment is applied, the size of the fibers decreases significantly suggesting a higher removal of pectin/lignin traces liberating the inner cellulose.

This behavior is corroborated in the images obtained by SEM, where it can be appreciated in more detail with the samples of the material before and after the alkaline and hydrolysis treatments. Figure 2a, b show the morphology of the raw material in which rib-like structures are present along with sheets-like structure (platelets). In a previous article, it was determined in the presence of methylene blue, that the sheets and fibers are covered with lignin [23]. Figure 2(c) shows the main diameter and size distribution of the fibers contained in the raw material which are mostly in the range of 3.2–3.5 µm. After the bleaching/alkaline treatment, it can be observed an important removal of the pectin/lignin that wrapped the fibers of the raw material (Fig. 2d, e). A size decrease in diameter occurs now being in the range of 2.4–3.0 µm. After hydrolysis was performed (Fig. 2g–i) fibers totally lose the rib-like structure they had originally and they display a random orientation. Figure 2h shows an isolated fiber without impurities on the surface. The size decreased once again to be in the range of 1.6–2.0 µm.

More detailed images of the hydrolysis treated samples are shown in Fig. 3a–d in which two particles were analyzed by OM and SEM. When making a zoom within and at the edges of the particles, Figs. 3e, f, a matrix of nanofibers corresponding to nanocellulose can be seen. In Fig. 3e an isolated fiber shows parallel arrays of nanofibrils, which is a characteristic morphology in most of the micro cellulose sources [26], while Fig. 3f shows randomly arranged nanofibrils embedded in an amorphous cellulose matrix [22], which is characteristic of the two-dimensional nanocellulose [7]. The color-depicted (blue) in Fig. 3a, b

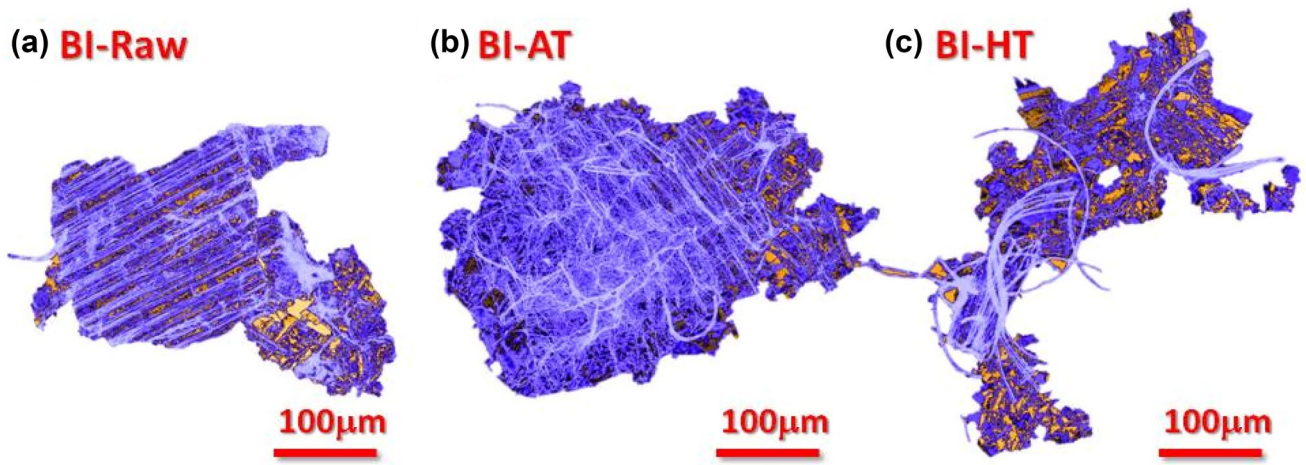

Fig. 1 Images obtained by OM corresponding to **a** Raw Material, **b** Alkalinization Treated Sample and **c** Hydrolysis Treated Sample

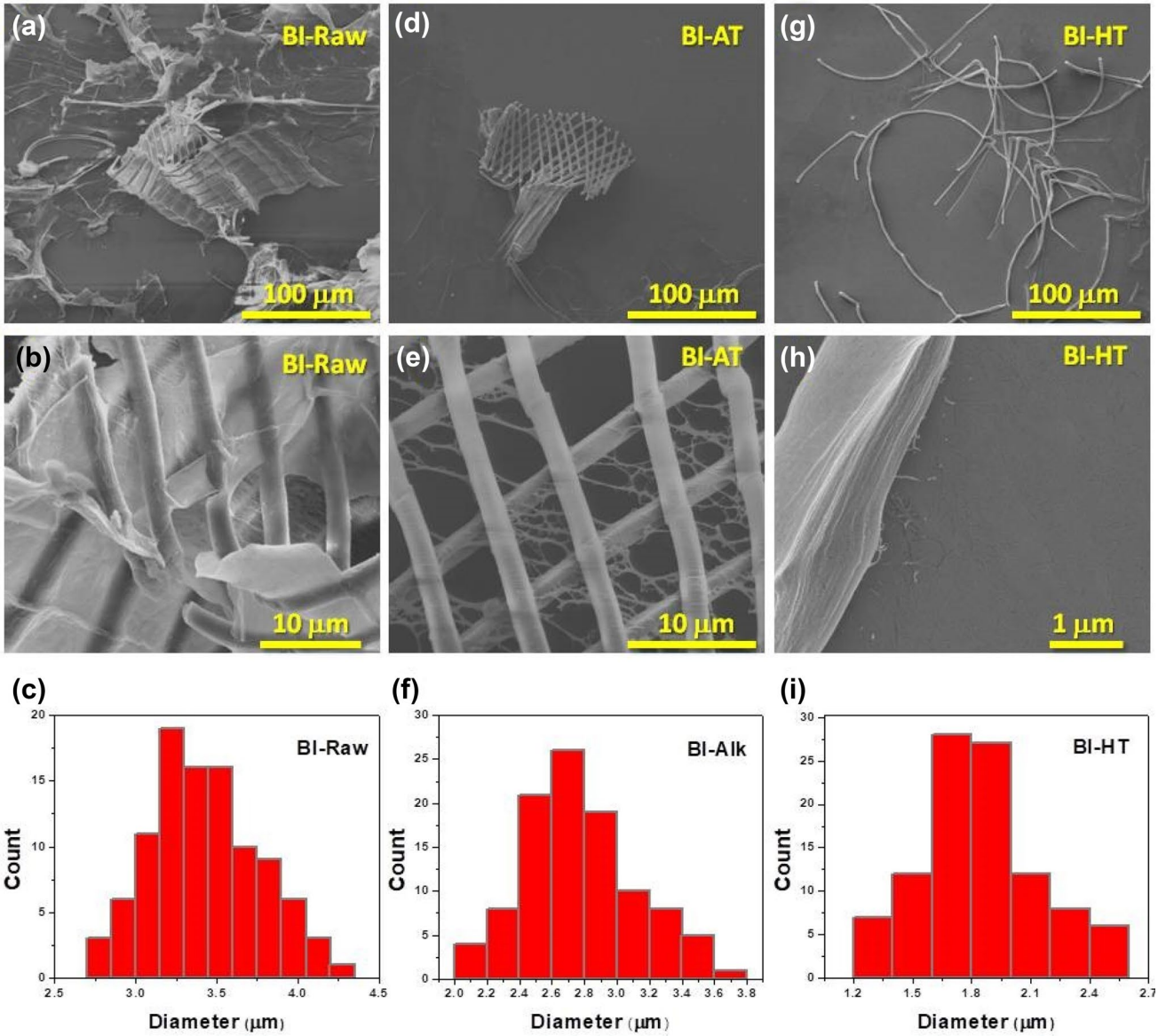

Fig. 2 SEM Images of **a**, **b** Raw Material, **c**, **d** Alkalinization Treated Sample, **g**–**h** Hydrolysis Treated Sample. The figures showed below the SEM Images **c**, **f**, and **i** corresponds to their respective fiber diameter size distribution

is caused by the light interaction with the nanoparticle, which can be observed due to the light interference, probing that the platelet has a thickness ≤ 100 nm. This behavior was previous described in detail by Chavez-Guerrero et al. [22], using a nanoplatelet isolated from *Agave salmiana*, showing that there is only dependence of thickness, regardless of the cellulose source. It can be appreciated that the cellulose fibril does not show any characteristic color, because of the size (≈2 µm), such difference in size can be appreciated in detail in Fig. 3c–f, corroborating previous reports [23].

ATR Spectroscopy

The ATR spectroscopic analyses of the raw material, alkaline treated and the hydrolyzed samples show a series of compositional changes through the chemical treatments. The spectrum of the raw material exhibits a prominent peak at 1725 cm^{-1} which can be ascribed either to stretch modes of C=O bonds of the ester groups of hemicellulose or to the ester bonds of the carboxylic groups of lignin, pectin and/or hemicelluloses. Raw material spectra also show a peak at 1513 cm^{-1} attributed to stretching of the –C=C–bonds of the aromatic bonds of lignin.

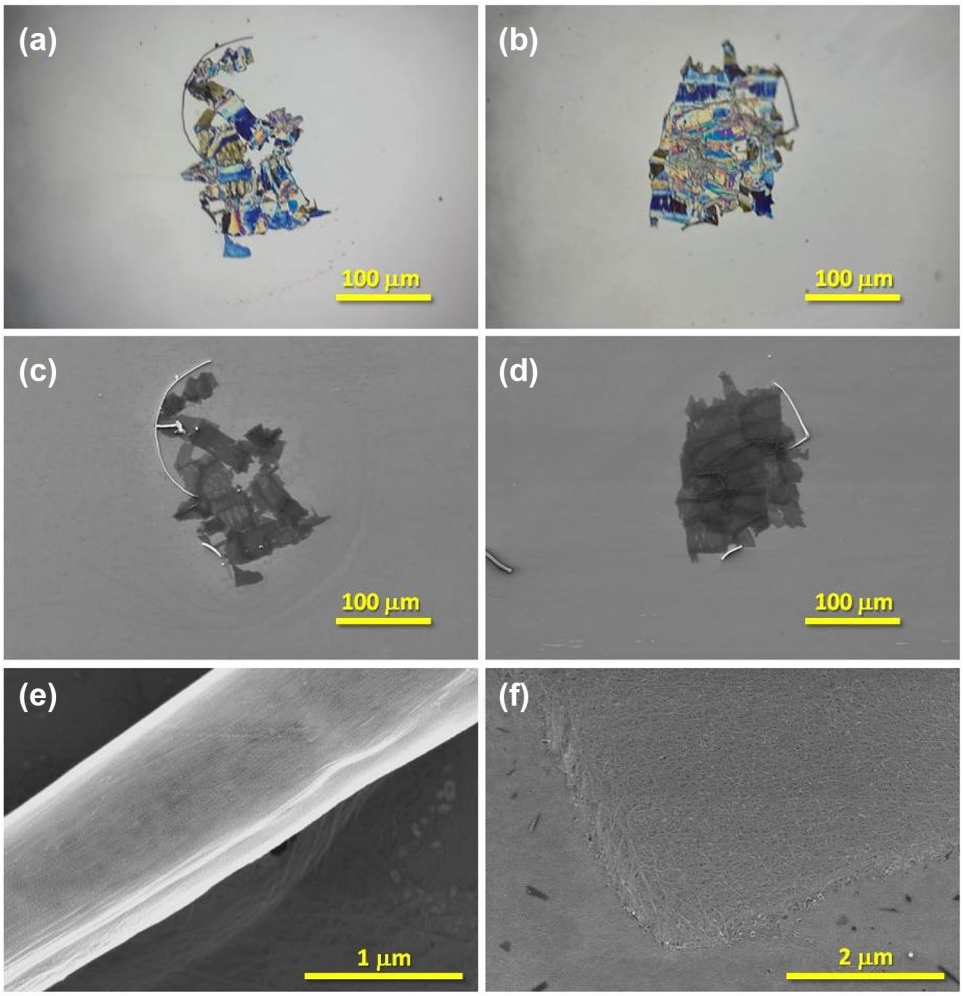

Fig. 3 Two Hydrolyzed Samples (BI-HT) analyzed by OM **a**, **b** and SEM **c**–**f**

The peaks described above cannot be found in the spectra of the alkaline and hydrolyzed samples, suggesting the elimination of most of the hemicellulose, pectin and lignin contained in the fibers throughout the chemical treatments. The peak at 1424 cm^{-1} corresponds to the bending of $–CH_2–$ bonds. Multiple peaks can be observed in the range of 1200–950 cm^{-1} which can be attributed to the stretching vibration of –C–O– bonds [27] being the peak located at 1030 cm^{-1} the most prominent. The hydrolyzed sample exhibits more intense and a major number of peaks in the 1200–950 cm^{-1} range than the raw material due to its major content of cellulose. The band located at 897 cm^{-1} is typical of the structure of cellulose and represents the deformation of glycosidic –C–H bonds with a ring vibration contribution of bending vibrations of –O–H bonds which are distinctive of β-glycosidic bondings among anhydroglucose units in cellulose [28]. That peak is sharper and more intense in the chemically treated samples. The large peak located among 3600–3000 cm^{-1} corresponds to the –O–H groups and varies slightly from the raw material to the treated samples which implies that the moisture content differs as a result of cellulose chain ruptures during hydrolysis treatment.

X-Ray Diffraction (XRD)

Hydrogen bonding interactions and Van der Waals forces between adjacent molecules of cellulose cause its crystallinity [29]. Figure 5 shows the XRD patterns of the samples. The diffraction peaks located at $2\theta = 22°$ and 15.58° represents the typical cellulose I diffractograms [30]. The patterns of the treated samples have more intense peaks than the raw sample which suggests a higher degree of crystallinity due to a higher amount of cellulose and the reduced amount of pectin and lignin which could shield the pattern peaks of cellulose. Thereby, the increment in the overall order of the chemical treated fibers can be ascribed to significant removal of hemicellulose, pectin and lignin traces in the course of the acid treatment to finally isolate the cellulose I, also previously seen in Fig. 4.

Crystallinity was determined by the peak height method described in Eq. (1). The crystallinity index (CrI) varies

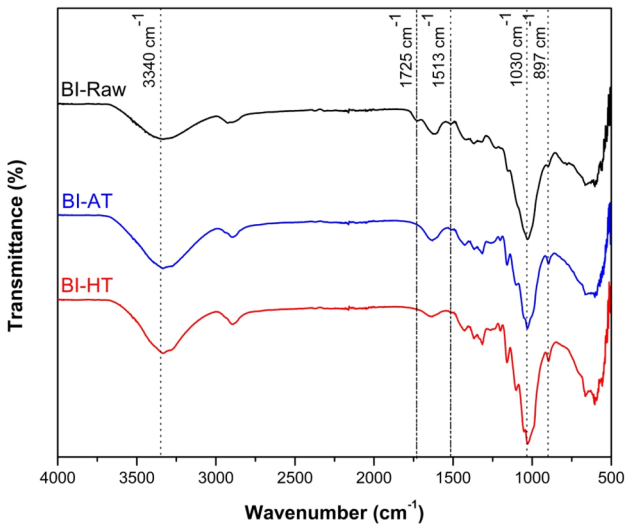

Fig. 4 ATR Analysis of Raw and Chemical Treated Samples

from each sample increasing from 62.09% for the raw sample, 72.97% after alkaline treatment finally reaching 78.05% in the hydrolyzed sample. The crystallinity of the treated samples is comparable to the work made by Mueller et al. [14]. It has been reported that when highly crystalline bacterial cellulose is added as reinforcement the mechanical properties of nanocellulose will increase, creating a super-strong network structure [31]. Then, the raise in the cellulose fibers crystallinity was expected to enhance the rigidity and strength of the films, reinforcing the all-cellulose films, as shown Fig. 6.

Tensile Strength Tests

The tensile stress–strain curves of the films obtained by alkaline and hydrolysis treatments are compared in Fig. 6. It can be observed that the films made with hydrolyzed can withstand greater amounts of stress and also can be deformed twice more than the alkaline samples due to its major amount of nanocellulose which increases the number of bonds within the film. The microfibers are entangled in BI-AT, attached by non-cellulosic materials (Fig. 2) which explains the rigidity of the samples, as shown in Fig. 6. After the hydrolysis, the fibers got loose (the reinforcing phase) increasing twice the strength of the film. While the cellulose suspension during the casting remains liquid, the rearrangement of the fibers and nanoplatelets will be possible (nematic self-ordering), improving the mechanical properties of the BI-HT film.

The results agree with the observations of Ververis et al. [32] who state that tensile strength is directly proportional to cellulose content. Gindl et al. synthesized acetate butyrate films reinforced with cellulose reaching up to 128.9 MPa in

Table 1 Mechanical properties of cellulose films

Sample	Average tensile strength (F_{max}) (MPa)	Average strain at F_{max} (%)
BI-AT	80.40	2.95
BI-HT	181.33	6.43

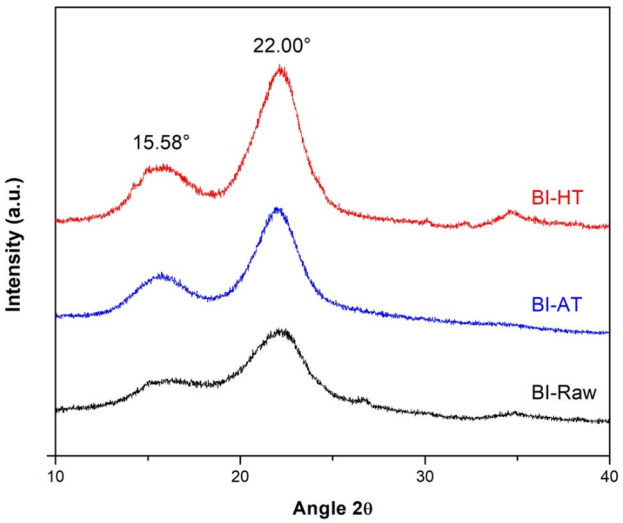

Fig. 5 Diffraction patterns of banana pseudostem samples

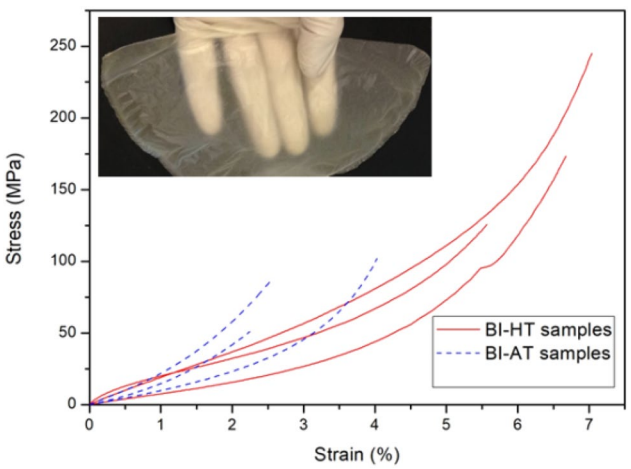

Fig. 6 Tensile test results of BI-AT and BI-HT samples (shown in the inset)

tensile strength with an average maximum strain of ≈3.5% [33]. Besides, Eichhorn et al. made cellulose films from different samples of regenerated cellulose half of which not exceeded 6% of strain [34]. Also, reports on dissolved/regenerated laminar all-cellulose films [31] have shown a wide

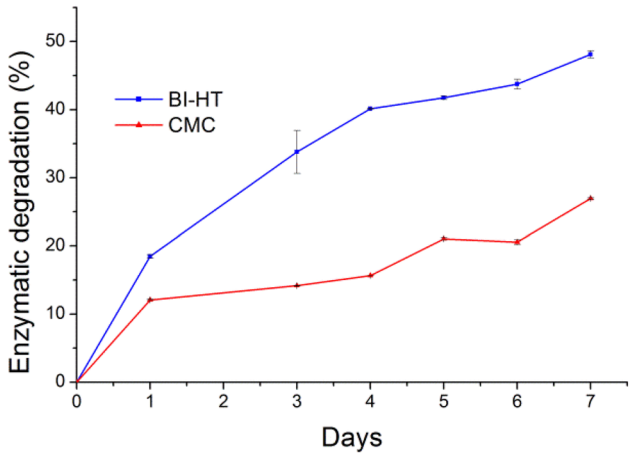

Fig. 7 Enzymatic hydrolysis of the samples BI-HT compared to commercial cellulose (CMC)

range of properties, with values up to 106 MPa of tensile strength, which is similar to our results. Table 1 summarizes the data obtained from the tests.

Then, the increase in the tensile strength from alkaline to hydrolyzed samples can be attributed to: (i) the smaller fibers (Fig. 2i) makes tougher films because they create tighter networks with more junction points; (ii) the number of defect points of microfibers such as slits and pits were removed by downsizing fibers increasing the crystallinity index (Fig. 5), resulting in a delayed breakup of the samples.

Polymers degrade in several years, leaving plastic microparticles in soil and water around the world. But cellulose can be decomposed in a few months, since several organisms, mainly fungi, use it as a source of energy through specific enzymes to obtain the sugars whit in the cellulose fibers or platelets [4, 35]. So, this material can be considered edible [36], acting as a dietary fiber in the case it is consumed by accident once disposed of.

In nature, *Trichoderma longibrachiatum* utilizes an enzymatic cocktail to degrade decaying biomass, recycling cellulose to restore soil nutrients. The effect of *Trichoderma longibrachiatum* on banana pseudostem cellulose can be observed in Fig. 7, indicating 50% degradation in only 7 days, producing reducing sugars as a residue. In both cases, a high rate of hydrolysis can be observed in the first 24 h, which is expected, since amorphous cellulose is consumed first [22]. Then a steady degradation rate can be observed for the next 6 days in the case of BI-HT, where we hypostatized that the cellulose nanoplatelets were hydrolyzed, instead of the highly ordered fibers. This can be corroborated by the CMC behavior under the same conditions since CMC is composed entirely of fibers (cotton linters), where the hydrolysis rate is clearly lower, almost half after 7 days.

Based on the results (Figs. 6 and 7), these films show great potential in the packaging industry, where even a small substitution of the synthetic polymers will diminish the solid waste problem, reducing environmental concerns [36]. Also, the cellulose that integrates the films was not previously dissolved, just isolated; such a process allows the use of fewer chemical reactants or the use of expensive procedures. Then, the all-cellulose films produced in this report show great potential for several applications [36] in the food and packaging industry, ensuring a reduced time to degrade at the end of the useful life.

Conclusions

A substantial increase of crystallinity of banana pseudostem fibers was observed after chemical treatment which is attributed to the removal of amorphous non-cellulosic materials, e.g. lignin, hemicellulose or pectin. FTIR and electronic microscope observations confirm the removal of the abovementioned species. Free-standing films made of cellulose nanoplatelets and cellulose fibers showed a crystallinity index of 78.05, which can resist ≈ 180 MPa of stress with 6% of average strain. Tensile tests made on the films shown good mechanical properties which gave them great potential in diverse applications as substitutes for polymers in the food or packaging industry. Downsizing fibers from micro to nanoscale reduces the number of defects within the nanofibrils, increasing their resistance because of its greater number of joints within the cellulose matrix (cellulose nanoplatelets). Finally, we demonstrated the feasibility of producing reducing sugars through enzymatic hydrolysis, which can be an indirect and rapid way to determine the biodegradability of such biopolymers in a determined time.

Acknowledgements The authors want to thank Dr. Ophélie Trussart from the Center for Research and Innovation in Aeronautical Engineering (CIIIA) of Universidad Autónoma de Nuevo León (UANL) for the facilities provided for ATR characterization. The authors want to thank the program PAICYT-UANL for the funding provided to develop the present project.

Compliance with ethical standards

Conflict of interest All authors declare no conflicts of interest.

References

1. Luckachan, G.E., Pillai, C.K.S.: Biodegradable polymers-a review on recent trends and emerging perspectives. J. Polym. Environ. **19**, 637–676 (2011)
2. Narancic, T., Cerrone, F., Beagan, N., et al.: Recent advances in bioplastics: application and biodegradation. Polymers **12**, 920 (2020)
3. Bar-On, Y.M., Philips, R., Milo, R.: The biomass distribution on Earth. PNAS **115**, 6506–6511 (2018)

4. Chen, C.C., Dai, L., Ma, L., et al.: Enzymatic degradation of plant biomass and synthetic polymers. Nat. Rev. Chem. **4**, 114–126 (2020)
5. Zhou, C.H., Xia, X., Lin, C.X., et al.: Catalytic conversion of lignocellulosic biomass to fine chemicals and fuels. Chem. Soc. Rev. **40**, 5588–5617 (2011)
6. Ahn, Y., Lee, S.H., Kim, H.J., et al.: Electrospinning of lignocellulosic biomass using ioni liquid. Carbohydr. Polym. **88**, 395–398 (2012)
7. Chávez-Guerrero, L., Sepúlveda-Guzmán, S., Rodríguez-Liñan, C., et al.: Isolation and characterization of cellulose nanoplatelets from the parenchyma cells of *Agave salmiana*. Cellulose **24**, 3741–3752 (2017)
8. Zhang, J., Luo, N., Wan, J., et al.: Directly converting agricultural straw into all-biomass nanocomposite films reinforced with additonal in situ-retained cellulose nanocrystals. ACS Sustain. Chem. Eng. **5**(6), 5127–5133 (2017)
9. Malainine, M.E., Mahrouz, M., Dufresen, A.: Thermoplastic nanocomposites based on cellulose microfibrils from *Opuntia ficus-indica* parenchyma cell. Compos. Sci. Technol. **65**(10), 1520–1526 (2005)
10. Fortunati, E., Puglia, D., Monti, M., et al.: Cellulose nanocrystals extracted from okra fibers in PVA nanocomposites. J. Appl. Polym. Sci. **128**(5), 3220–3230 (2013)
11. Zuluaga, R., Putaux, J.L., Restrepo, A., et al.: Cellulose microfibrils from banana farming residues: isolation and characterization. Cellulose **14**, 585–592 (2007)
12. Kamdem, I., Hiligsmann, S., Vanderghem, C., et al.: Enhanced biogas production during anaerobic digestion of steam-pretreated lignocellulosic biomass from Williams Cavendish banana plants. Waste Biomass Valoriz. **9**, 175–185 (2018)
13. FAO. 2020. Banana Market Review: Preliminary Results 2019. Rome. Accessed 03 December 2020. http://www.fao.org/publications/card/es/c/CA7567EN/
14. Mueller, S., Weder, C., Foster, E.J.: Isolation of cellulose nanocrystals from pseudostems of banana plants. RSC Adv. **4**, 907–915 (2014)
15. Fitri Faradilla, R.H., Lee, G., Rawal, A., et al.: Nanocellulose characteristics from the inner and outer layer of banana pseudostem prepared by TEMPO-mediated oxidation. Cellulose **23**, 3023–3037 (2016)
16. Khawas, P., Deka, S.C.: Isolation and characterization of cellulose nanofibers from culinary banana peel using high-intensity ultrasonication combined with chemical treatmen. Carbohydr. Polym. **137**, 608–616 (2016)
17. Phantong, P., Karnjanakom, S., Reubroycharoen, P., et al.: A facile one-step way fro extraction of nanocellulose with high yield by ball milling with ionic liquid. Cellulose **24**, 2083–2093 (2017)
18. Tibolla, H., Pelissari, F.M., Martins, J.T., et al.: Cellulose nanofibers produced from banana peel by chemical and mechanical treatments: characterization and cytotoxicity assessment. Food Hidrocoll. **75**, 192–201 (2018)
19. Cherian, B.M., Pothan, L.A., Nguyen-Chung, T., et al.: A novel method for the synthesis of cellulose nanofibril whiskers from banana fibers and characterization. J. Agric. Food Chem. **56**(14), 5617–5627 (2008)
20. Deepa, B., Abraham, E., Cherian, B.M., et al.: Structure, morphology and thermal characteristics of banana nanofibers obtained by steam explosion. Bioresour. Technol. **102**, 1988–1997 (2011)
21. ISO/TR 18401:2017.: Nanotechnologies—Plain Language Explanation of Selected Terms from the ISO/IEC 80004 Series. https://www.iso.org/obp/ui/#iso:std:iso:tr:18401:ed-1:v1:en. Accesed 03 December 2020.
22 Chávez-Guerrero, L., Silva-Mendoza, J., Toxqui-Terán, A., et al.: Direct observation of endoglucanase fibrillation and rapid thickness identification of cellulose nanoplatelets using constructive interference. Carbohydr. Polym. **254**, 117463 (2020)
23. Chávez-Guerrero, L., Vazquez-Rodriguez, S., Salinas-Montelongo, J.A., et al.: Preparation of all-cellulose composites with optical transparency using the banana pseudostem as a raw material. Cellulose **26**(6), 3777–3786 (2019)
24. Segal, L., Creely, J.J., Martin, A.E., et al.: An empirical method for estimating the degree of crystallinity of native cellulose using the X-ray diffractometer. Text. Res. J. **29**(10), 786–794 (1959)
25. Miller, G.L.: Use of dinitrosalicylic acid reagent for determination of reducing sugar. Anal. Chem. **31**(3), 426–428 (1959)
26. Chávez-Guerrero, L., Esneider, M., Bonilla, J., Toxqui-Terán, A.: Eco-friendly extraction of fibrils with hierarchical structure assisted by freeze-drying using agave salmiana leaves as a raw material. Fibers Polym. **21**, 66–72 (2020)
27. Alemdar, A., Sain, M., et al.: Biocomposites from wheat straw nanofibers: morphology, thermal and mechanical properties. Compos. Sci. Technol. **68**(2), 557–565 (2008)
28. Elanthikkal, S., Gopalakrishnapanicker, U., Varghese, S., et al.: Cellulose microfibres produced from banana plant wastes: isolation and characterization. Carbohydr. Polym. **80**(3), 852–859 (2010)
29. Zhang, Y.H., Lynd, L.R.: Toward an aggregated understanding of enzymatic hydrolysis of cellulose: noncomplexed cellulase systems. Biotechnol. Bioeng. **88**(7), 797–824 (2004)
30. Bondeson, D., Mathew, A., Oksman, K.: Optimization of the isolation of nanocrystals from microcrystalline cellulose by acid hydrolysis. Cellulose **13**, 171 (2006)
31. Li, J., Nawaz, H., Wu, J., et al.: All-cellulose composites based on the self-reinforced effect. Compos. Commun. **9**, 42–53 (2018)
32. Ververis, C., Georghiou, K., Christodoulakis, N., et al.: Fiber dimensions, lignin and cellulose content of various plant materials and their suitability for paper production. Ind. Crop. Prod. **19**(3), 245–254 (2004)
33. Gindl, W., Keckes, J.: Tensile properties of cellulose acetate butyrate composites reinforced with bacterial cellulose. Compos. Sci. Technol. **64**(15), 2407–2413 (2004)
34. Eichhorn, S.J., Sirichaisit, J., Young, R.J.: Deformation mechanisms in cellulose fibres, paper and wood. J. Matter. Sci. **36**, 3129–3135 (2001)
35. A. Karppinen. Biodegradability of cellulose fibrils. https://www.exilva.com/blog/biodegradability-of-cellulose-fibrils. Accessed 27 July 2020.
36. Sothornvit, R., Pitak, N.: Oxygen permeability and mechanical properties of banana films. Food Res. Int. **40**(3), 365–370 (2007)